

Transport responses from rate of decay and scattering processes in the Nambu–Jona-Lasinio model

Sabyasachi Ghosh¹, Fernando E. Serna^{2,3}, Aman Abhishek^{4,5}, Gastão Krein², Hiranmaya Mishra⁴

¹ *Indian Institute of Technology Bhilai, GEC Campus, Sejbahar, Raipur 492015, Chhattisgarh, India*

² *Instituto de Física Teórica, Universidade Estadual Paulista,*

Rua Dr. Bento Teobaldo Ferraz, 271, 01140-070 São Paulo, SP, Brazil

³ *Instituto Tecnológico de Aeronáutica, DCTA, 12228-900 São José dos Campos, SP, Brazil*

⁴ *Theory Division, Physical Research Laboratory, Navrangpura, Ahmedabad 380 009, India and*

⁵ *Indian Institute of Technology, Gandhinagar-382355, Gujarat, India*

We have calculated quark and anti-quark relaxation time by considering different possible elastic and inelastic scatterings in the medium. Comparative role of these elastic and inelastic scatterings on different transport coefficients are explored. The quark-meson effective interaction Lagrangian density in the framework of Nambu–Jona-Lasinio model is used for calculating both type of scatterings. Owing to a kinetic threshold, inelastic scatterings can only exist beyond the Mott line in temperature and chemical potential plane, whereas elastic scatterings occur in the entire plane. Interestingly, the strength of inelastic scatterings near and above Mott line becomes so strong that medium behaves like a perfect fluid, in that all transport coefficients become very small.

PACS numbers:

I. INTRODUCTION

The study of transport coefficients at finite temperature and baryon density of strongly interacting matter is a subject of current interest in different contexts. At high baryon density and low temperature, transport coefficients are relevant for the study of an array of phenomena in compact stars [1, 2], and at high temperatures and low densities, they are relevant in the context of heavy-ion collisions [3], mainly in connection with the strongly-coupled nature of the quark-gluon plasma (QGP) produced in those collisions [4]. A weakly interacting QGP was a natural expectation at high temperatures since the early days of QCD because of its asymptotic freedom property. However, that expectation seems not to be realized at current collider energies, as the data on such collisions performed at the Relativistic Heavy Ion Collider (RHIC) and the Large Hadron Collider (LHC) can be described in a first approximation by low-viscosity hydrodynamics, a feature that implies a strongly-coupled medium. Here, the most relevant transport coefficient is shear viscosity, η . Still in the context of heavy-ion collisions, another important transport coefficient is electrical conductivity, σ . This coefficient is relevant e.g. for describing the low mass dimuon enhancement [5, 6] measured by the NA60 collaboration [7] at CERN, a subject related to chiral symmetry restoration. Similar to electrical conductivity, thermal conductivity, κ , is still another relevant transport coefficient. The effect of thermal conductivity on the hydrodynamical evolution of the QGP can not be neglected in situations of high baryon density, as thermal conduction takes place in the medium.

Currently, transport coefficients of the QGP can not be calculated directly from QCD using analytical methods. Lattice QCD is delivering its first results on these quantities. For example, results for the electrical conductivity have been reported in Refs [8–14], but the results

still contain large uncertainties. Extraction of these coefficients from lattice simulations are very challenging because because they are Minkowski-space dynamical quantities and the simulations are performed in Euclidean space—Ref. [15] is a recent review on the subject. Effective models of QCD have been extensively used in the recent years and have been a fundamental source of a great deal of insight on these coefficients. By far, shear viscosity η has attracted most of the attention because of its central role in signalling the strongly coupled nature of the QGP—the literature is too extensive to be reviewed here and but a selective list of references, closely related to the present work, can be found in Refs. [16–30]. Regarding σ , recent calculations find contradictory results for hadronic matter (pion gas): while Ref. [31] finds the ratio σ/T increasing with T , Refs. [16, 32, 33] find it decreasing with T . Calculations using models intended to describe simultaneously hadronic and partonic matter, like the Parton-Hadron-String-Dynamics model [34] and the Nambu-Jona-Lasino (NJL) model [17] predict $\sigma(T)/T$ decreasing with T in hadronic phase and increasing in the partonic phase. A calculation employing a holographic model [35] and others employing transport simulations [36, 37] find $\sigma(T)/T$ decreasing in the partonic phase. Regarding thermal conductivity, its has been addressed in a few references using different models [16–20, 38–43].

Dissipation is a dynamical effect that plays an important in defining the properties of transport coefficients. In a quasi-particle description of the strongly interacting medium, the main source of dissipation are the microscopic elastic and inelastic scattering processes involving the quasi-particles. In most of the models employed to date, the quasi-particles are massive constituent quarks and scalar-isoscalar (σ) and pseudoscalar-isovector (π) mesons, the degrees of freedom associated with the dynamical breaking of chiral symmetry. Earlier [25, 26] and

more recent [17, 20, 28] works have investigated the effects of $2 \leftrightarrow 2$ type of elastic quark-quark scatterings. More recently, Refs. [21–24, 29, 30] have investigated the contributions of inelastic quark-meson processes of the type $1 \leftrightarrow 2$, finding that those processes play an important role within a narrow temperature window near but above the Mott temperature, a temperature beyond which the pionic bound state delocalizes into its constituents. However, to date no work has investigated the joint effect of the $2 \leftrightarrow 2$ and $1 \leftrightarrow 2$ types of scatterings. The present work provides such an investigation within the dynamical framework of the Nambu–Jona-Lasinio (NJL) model. This model allows us, in particular, to calculate the $2 \leftrightarrow 2$ and $1 \leftrightarrow 2$ processes within the same underlying model and, in addition, to take into account in a self-consistent manner the dynamics of chiral symmetry restoration as a function of temperature and baryon density. We find, in particular, that the self-consistency has a dramatic effect on the transport coefficients.

The paper is organized as follows. In the next section, we address the formalism part, where we define the model and present the standard expressions of the transport coefficients within the Kubo formalism. In section III, we derive the expressions of the thermal widths to the $2 \leftrightarrow 2$ and $1 \leftrightarrow 2$ processes. Our numerical results are presented in section IV. Finally, section V present a summary and present the main conclusions of the work.

II. FORMALISM

We employ the Kubo formalism [44, 45] to compute the transport coefficients η (shear viscosity), σ (electrical conductivity) and κ (thermal conductivity). In this formalism, the transport coefficients are given in terms of correlation functions of operators involving components of the energy-momentum tensor $T_{\mu\nu}$, the quark-number N_μ and the electrical J_μ currents. Here, it is assumed a system in the hydrodynamical regime, where relaxation time of the constituents is much shorter than the life time of the whole system. Under such an assumption, the medium is not far from equilibrium and in the evaluation of statistical averages of the energy-momentum tensor and currents only linear terms in spacetime gradients of local thermodynamical parameters (like temperature, velocity field, etc.) are retained; this is the linear response theory and leads to expressions for transport coefficients that coincide with those derived within the relaxation time approximation [46].

The energy-momentum tensor is given in terms of the Lagrangian density \mathcal{L} of the model as

$$T^{\mu\nu} = -g^{\mu\nu}\mathcal{L} + \frac{\partial\mathcal{L}}{\partial(\partial_\mu\psi)}\partial^\nu\psi = g^{\mu\nu}\mathcal{L} + i\bar{\psi}\gamma^\mu\partial^\nu\psi. \quad (1)$$

The quark-number N_μ and electrical J_μ currents are given by

$$N_\mu = \bar{\psi}\gamma_\mu\psi, \quad J_\mu = \bar{\psi}\hat{Q}\gamma_\mu\psi, \quad (2)$$

where \hat{Q} is the charge matrix given in terms of the elementary electric charge e as

$$\hat{Q} = e \begin{pmatrix} 2/3 & 0 \\ 0 & -1/3 \end{pmatrix}. \quad (3)$$

The transport coefficients are given in terms of correlation functions of these quantities as

$$\begin{pmatrix} \eta \\ \sigma \\ \kappa \end{pmatrix} = \lim_{q_0, |\mathbf{q}| \rightarrow 0^+} \frac{1}{q^0} \begin{pmatrix} \frac{1}{20}A_\eta(q^0, \mathbf{q}) \\ \frac{1}{6}A_\sigma(q^0, \mathbf{q}) \\ \frac{-\beta}{6}A_\kappa(q^0, \mathbf{q}) \end{pmatrix}, \quad (4)$$

with $\beta = 1/T$, where T is the temperature, and $A_\eta(q)$, $A_\sigma(q)$ and $A_\kappa(q)$ are the spectral functions:

$$A_\eta(q) = \int d^4x e^{iq \cdot x} \langle [\pi^{ij}(x), \pi^{ij}(0)] \rangle_\beta, \quad (5)$$

$$A_\sigma(q) = \int d^4x e^{iq \cdot x} \langle [J_i(x), J^i(0)] \rangle_\beta, \quad (6)$$

$$A_\kappa(q) = \int d^4x e^{iq \cdot x} \langle [\mathcal{T}_i(x), \mathcal{T}^i(0)] \rangle_\beta, \quad (7)$$

$$(8)$$

where

$$\pi^{ij}(x) = T^{ij}(x) - \frac{1}{3}\delta^{ij}T^k_k, \quad (9)$$

$$\mathcal{T}^i(x) = -T^{i0}(x) - q N^i(x), \quad (10)$$

with q being the enthalpy per particle, given in terms of the energy density ϵ , the pressure P and net baryon density ρ of the system as $q = (\epsilon + P)/\rho$. In Eqs. (5)–(7), $\langle (\dots) \rangle_\beta$ denotes an appropriate thermal average. We are also interested in presenting results for the ratio η/s , where s is the entropy density, given in terms of ϵ , P and ρ as $s = (\epsilon + P - \mu\rho)/T$, where μ is the baryon chemical potential.

We utilise the NJL model to derive the correlation functions and the thermodynamic functions. The Lagrangian density of the model for u and d flavors is given by [49]

$$\mathcal{L} = \bar{\psi}(i\partial\!\!\!/ - m_Q)\psi + G [(\bar{\psi}\psi)^2 + (\bar{\psi}i\gamma^5\boldsymbol{\tau}\psi)^2], \quad (11)$$

where m_Q is the current-quark mass matrix, which is diagonal with elements m_u and m_d , and $\boldsymbol{\tau} = (\tau^1, \tau^2, \tau^3)$ are the flavor Pauli matrices. The model is solved in the quasi-particle approximation or, equivalently, in the leading-order approximation in the $1/N_c$ expansion, where $N_c = 3$ is the number of colors. This approximation is also equivalent to the traditional Hartree approximation of many-body theory. In this approximation, the thermal spectral functions and the thermodynamic functions are given in terms of the quark propagator.

We employ the formalism of real-time thermal field theory (RTF) to evaluate the correlation functions and

thermodynamic functions. In RFT, the two point function of any field-theoretic operator has a 2×2 matrix structure reflecting the time ordering with respect to a contour in the complex plane [47]. The relevant matrix can be diagonalized in terms of a single analytic function, which determines completely the dynamics of the corresponding two-point function — for details, see Ref. [48].

For example, when neglecting dissipative effects, the 11 component of the quark propagator in the quasi-particle approximation to the NJL model is given by

$$S_{11}(k) = (\not{k} + M_Q) D_{11}(k), \quad (12)$$

with $k = (k_0, \mathbf{k})$ and

$$D_{11}(k) = \frac{-1}{k_0^2 - (\omega_Q^k)^2 + i\varepsilon} - 2\pi i \omega_Q^k \delta(k_0^2 - (\omega_Q^k)^2) [n_Q(\mathbf{k})\theta(k_0) + n_{\bar{Q}}(\mathbf{k})\theta(-k_0)], \quad (13)$$

where $\theta(k_0)$ is the step function, $\omega_Q^k = (\mathbf{k}^2 + M_Q^2)^{1/2}$, with M_Q being the constituent quark mass of a given flavor (u or d), given by the solution of the gap equation [49]

$$M_Q = m_Q + 4N_f N_c G \int_0^\Lambda \frac{d^3 \mathbf{k}}{(2\pi)^3} \frac{M_Q}{\omega_Q^k} [1 - n_Q(\mathbf{k}) - n_{\bar{Q}}(\mathbf{k})], \quad (14)$$

where $N_f = 2$ and $N_c = 3$ the numbers of flavor and colors, and $n_Q(\mathbf{k})$ and $n_{\bar{Q}}(\mathbf{k})$ are respectively the Fermi-Dirac distributions of quarks and antiquarks:

$$n_Q(\mathbf{k}) = \frac{1}{e^{\beta(\omega_Q^k - \mu)} + 1}, \quad n_{\bar{Q}}(\mathbf{k}) = \frac{1}{e^{\beta(\omega_Q^k + \mu)} + 1}. \quad (15)$$

Dissipative effects due to fluctuations introduce an imaginary part in the quark self energy giving a thermal width Γ_Q , thereof modifying the quark propagator. Using the quark propagator modified by the width Γ_Q [48, 50], η , σ and κ can be readily obtained in the relaxation time approximation [18, 46] or from the one-loop Kubo expression [16, 32, 48]. Their expressions are given by

$$\eta = \frac{2N_F N_c \beta}{15} \int \frac{d^3 \mathbf{k}}{(2\pi)^3 \Gamma_Q} \left(\frac{\mathbf{k}^2}{\omega_Q^k} \right)^2 \{n_Q(\mathbf{k}) [1 - n_Q(\mathbf{k})] + n_{\bar{Q}}(\mathbf{k}) [1 - n_{\bar{Q}}(\mathbf{k})]\}, \quad (16)$$

$$\sigma = \left(\frac{2N_c \beta}{3} \right) \left(\frac{5e^2}{9} \right) \int \frac{d^3 \mathbf{k}}{(2\pi)^3 \Gamma_Q} \left(\frac{\mathbf{k}}{\omega_Q^k} \right)^2 \{n_Q(\mathbf{k}) [1 - n_Q(\mathbf{k})] + n_{\bar{Q}}(\mathbf{k}) [1 - n_{\bar{Q}}(\mathbf{k})]\}, \quad (17)$$

$$\kappa = \frac{2N_F N_c \beta^2}{3} \int \frac{d^3 \mathbf{k}}{(2\pi)^3 \Gamma_Q} \left(\frac{\mathbf{k}}{\omega_Q^k} \right)^2 \{(\omega_Q^k - q)^2 n_Q(\mathbf{k}) [1 - n_Q(\mathbf{k})] + (\omega_Q^k + q)^2 n_{\bar{Q}}(\mathbf{k}) [1 - n_{\bar{Q}}(\mathbf{k})]\}. \quad (18)$$

The explicit expression for the enthalpy h in the present model, together with those for other thermodynamic functions, are given the appendix. The calculation of the contribution of quark-meson fluctuations to Γ_Q requires meson masses m_M and quark-meson couplings g_{MQQ} , for $M = \sigma, \pi$. Their expressions in the quasi-particle approximation are well known in the literature [49], but repeat them here for completeness and setting the notation:

$$1 - 2G\Pi_M(\omega^2 = m_M^2) = 0, \quad g_{MQQ}^2 = \left[\frac{\partial \Pi_M(\omega^2)}{\partial \omega^2} \right]_{\omega^2 = m_M^2}^{-1}, \quad (19)$$

where $\Pi_M(\omega^2)$ is the proper polarization function

$$\Pi_M(\omega^2) = 2N_c N_f \int_0^\Lambda \frac{d^3 \mathbf{k}}{(2\pi)^3} \frac{F_M(\omega^2)}{\omega_Q^k} [1 - n_Q(\mathbf{k}) - n_{\bar{Q}}(\mathbf{k})], \quad (20)$$

with

$$F_\pi(\omega^2) = \frac{(\omega_Q^k)^2}{(\omega_Q^k)^2 - \omega^2/4}, \quad F_\sigma(\omega^2) = \frac{(\omega_Q^k)^2 - M_Q^2}{(\omega_Q^k)^2 - \omega^2/4}. \quad (21)$$

The integrals in Eq. (20) are evaluated as principal-value integrals when $\omega^2 > 4M_Q^2$.

For the same reasons, we present the expressions for the pressure P , the energy density ϵ , and baryon den-

sity ρ :

$$P = 2N_f N_c \int \frac{d^3 k}{(2\pi)^3} \frac{\mathbf{k}^2}{3\omega_Q^k} [n_Q(\omega_Q^k) + n_{\bar{Q}}(\omega_Q^k)], \quad (22)$$

$$\epsilon = 2N_f N_c \int \frac{d^3 k}{(2\pi)^3} \omega_Q^k [n_Q(\omega_Q^k) + n_{\bar{Q}}(\omega_Q^k)], \quad (23)$$

$$\rho = 2N_f N_c \int \frac{d^3 k}{(2\pi)^3} [n_Q(\omega_Q^k) - n_{\bar{Q}}(\omega_Q^k)]. \quad (24)$$

The entropy density s and enthalpy density h are related to the above quantities through the following relations:

$$s = \frac{\epsilon + P - \mu\rho}{T}, \quad (25)$$

$$h = \epsilon + P. \quad (26)$$

Another important thermodynamical quantity is the heat function q for each quark, defined by the ratio of enthalpy density to the net quark density, $q = h/\rho$. This quantity becomes divergent (unphysical) at $\mu = 0$, where net quark density vanishes.

III. COMPUTATION OF THERMAL WIDTHS

We evaluate the thermal width Γ_Q including contributions from $2 \leftrightarrow 2$ and $1 \leftrightarrow 2$ types of processes. The $2 \leftrightarrow 2$ processes refer to in-medium quark-antiquark and antiquark-antiquark scatterings mediated by σ and π exchanges, denoted generically by $QQ \leftrightarrow QQ$. The $1 \leftrightarrow 2$ processes refer to quark-meson fluctuations, denoted by $Q \leftrightarrow QM$.

For the two-flavor case, there are twelve possible $QQ \leftrightarrow QQ$ processes, whose matrix elements $\overline{M}_{QQ \leftrightarrow QQ}$ are written down explicitly in Refs. [20, 25, 26, 28], which we use for calculating the $\Gamma_{QQ \leftrightarrow QQ}$ contribution to the full width. Let us assume k and p (k' and p') for the initial (final) four-momenta in the scattering processes $Q(k) + Q(p) \rightarrow Q(k') + Q(p')$. Hence, the collisional width of a probe particle with momentum \mathbf{k} will be a function of the temperature T and chemical potential μ of the medium, with the momenta \mathbf{p} , \mathbf{k}' , \mathbf{p}' of the remaining participating particles in the scattering are integrated out, can be written as

$$\begin{aligned} \Gamma_{QQ \leftrightarrow QQ}(\mathbf{k}, T, \mu) &= \int \frac{d^3 \mathbf{p}}{(2\pi)^3 2\omega_Q^p} \frac{n_{Q/\bar{Q}}(\mathbf{p})}{1 + \delta_{kp}} \int \frac{d^3 \mathbf{k}'}{(2\pi)^3 2\omega_Q^{k'}} \int \frac{d^3 \mathbf{p}'}{(2\pi)^3 2\omega_Q^{p'}} [1 - n_{Q/\bar{Q}}(\mathbf{k}')] [1 - n_{Q/\bar{Q}}(\mathbf{p}')] \\ &\times (2\pi)^4 \delta^4(k + p - k' - p') |\overline{M}|_{QQ \leftrightarrow QQ}^2, \end{aligned} \quad (27)$$

where $1 + \delta_{k,p} = 2(1)$ for identical (nonidentical) quarks/antiquarks in the initial and final states. As in Ref. [28], we include a finite thermal width in the meson propagators in the expressions for $|\overline{M}|^2$.

Next, we consider the inelastic processes $Q \leftrightarrow QM$, in which a quark/antiquark can emit or absorb a thermalized meson from the medium. Their contributions $\Gamma_{Q \leftrightarrow QM}$ can be obtained from the Landau cut part of quark self-energy coming from quark-meson loops [52]. To evaluate the quark self-energy, we employ the quark-meson interaction Lagrangian densities [53],

$$\begin{aligned} \mathcal{L}_{\pi QQ} &= ig_{\pi QQ} \sum_{f=u,d} \bar{\psi}_f \gamma^5 \boldsymbol{\tau} \cdot \boldsymbol{\pi} \psi_f, \\ \mathcal{L}_{\sigma QQ} &= g_{\sigma QQ} \sum_{f=u,d} \bar{\psi}_f \sigma \psi_f, \end{aligned} \quad (28)$$

where the quark-meson couplings are obtained in the NJL model from Eq. (19). Given these, the imaginary part of the quark self-energy can be evaluated. Analyzing the branch cuts of this quark self-energy at finite temperature, one can easily find the quark pole $k = (\omega_Q^k, \mathbf{k})$ within the Landau-cut region $\mathbf{k} < k_0 < [\mathbf{k}^2 + (M_Q - m_M)^2]^{1/2}$ for $m_M > 2M_Q$, and write for $\Gamma_{Q \leftrightarrow QM}$ [48]:

$$\begin{aligned} \Gamma_{Q \leftrightarrow QM}(\mathbf{k}, T, \mu) &= -\frac{1}{2M_Q} \text{Tr} \left[(\not{k} + M_Q) \text{Im} \Sigma_{Q(QM)}^R(k) \right]_{k_0=\omega_Q^k} \\ &= \left[\int \frac{d^3 \mathbf{l}}{(2\pi)^3} \delta(k^0 + \omega_Q^l - \omega_M^u) \frac{n_Q(\mathbf{l}) + n_M(\mathbf{u})}{4\omega_Q^l \omega_M^u} L_{Q(QM)}(l^0 = -\omega_Q^l, \mathbf{l}, k) \right]_{k^0=\omega_Q^k}, \end{aligned} \quad (29)$$

where $\mathbf{u} = \mathbf{k} - \mathbf{l}$, $n_M(\mathbf{u})$ is the Bose-Einstein distribution

for mesons with energy $\omega_M^u = (\mathbf{u}^2 + m_M^2)^{1/2}$:

$$n_M(\mathbf{k}) = \frac{1}{e^{\beta\omega_M^u} - 1}, \quad (30)$$

and

$$L_{Q(Q\pi)}(l, k) = 3 \frac{4g_\pi^2}{2M_Q} [M_Q^2 - (k \cdot l)],$$

$$L_{Q(Q\sigma)}(l, k) = \frac{4g_\sigma^2}{2M_Q} [M_Q^2 + (k \cdot l)]. \quad (31)$$

The contributions from antiquarks are obtained from Eq. (29) by replacing $n_Q(\omega_Q^l)$ by $n_{\bar{Q}}(\omega_Q^l)$. Finally, we define average thermal widths $\Gamma_{Q \leftrightarrow Q Q}$ and $\Gamma_{Q(QM)}$ by the averages of $\Gamma_{Q \leftrightarrow Q Q}(\mathbf{k}, T, \mu)$ and $\Gamma_{Q \leftrightarrow Q M}(\mathbf{k}, T, \mu)$ over the thermal distributions:

$$\Gamma(T, \mu) = \frac{\int \frac{d^3 \mathbf{k}}{(2\pi)^3} \Gamma(\mathbf{k}, T, \mu) n_{Q/\bar{Q}}(\mathbf{k})}{\int \frac{d^3 \mathbf{k}}{(2\pi)^3} n_{Q/\bar{Q}}(\mathbf{k})}. \quad (32)$$

IV. RESULTS

The parameters of the model are fixed to obtain realistic values for the quark condensate $\langle \bar{u}u \rangle = \langle \bar{d}d \rangle = (-252 \text{ MeV})^3$, pion leptonic decay constant $f_\pi = 94 \text{ MeV}$ and the pion mass $m_\pi = 142 \text{ MeV}$. The parameters to be fixed are the current quark masses $m_Q = (m_u, m_d)$, the coupling G and the cutoff mass Λ . In present calculation, they are fixed to $m_Q = m_u = m_d = 5 \text{ MeV}$, $G\Lambda^2 = 2.14$, and $\Lambda = 653 \text{ MeV}$. At $T = 0$ and $\mu = 0$, the constituent quark and σ meson masses are $M_Q = M_u = M_d = 328 \text{ MeV}$ and $m_\sigma = 663 \text{ MeV}$. For completeness and clarity of presentation of our results on the transport coefficients, we present in Fig. 1 the T and μ dependences of the quark and meson masses and quark-meson couplings, and in Fig. 2 we present the thermodynamical functions.

Figure 1 reveals the well known facts that while the constituent quark mass M_Q and the $m_\sigma \simeq 2M_q$ and $g_{\pi QQ}$ drop significantly up to a pseudocritical temperature, the π mass and $g_{\sigma QQ}$ change very little with T . In addition, the pseudocritical temperature decreases when μ increases, reflecting the fact that both T and μ lead to a partial restoration of chiral symmetry. For values of T sufficiently higher than the pseudocritical temperature, the meson masses and quark-meson couplings become degenerate, reflecting the restoration of the approximate chiral symmetry of the Lagrangian.

Figure 2 presents the results for the thermodynamical functions h , ρ , q and s , normalized by the appropriate powers of T to obtain dimensionless ratios. To emphasize the effect of dynamical chiral symmetry breaking on those functions, they are also shown (red dotted lines) for massless quarks, i.e. they are calculated by setting $M_Q = 0$ in Eqs. (22)-(26). Clearly, at low (T, μ) values the effect of symmetry breaking is substantial and at high T one has the recovery of the Lagrangian symmetry. The heat function $q = h/\rho$ increases substantially for small values of μ because the net quark density ρ decreases as $\mu \rightarrow 0$. The thermal conductivity κ , being proportional q , increases substantially for small μ as well.

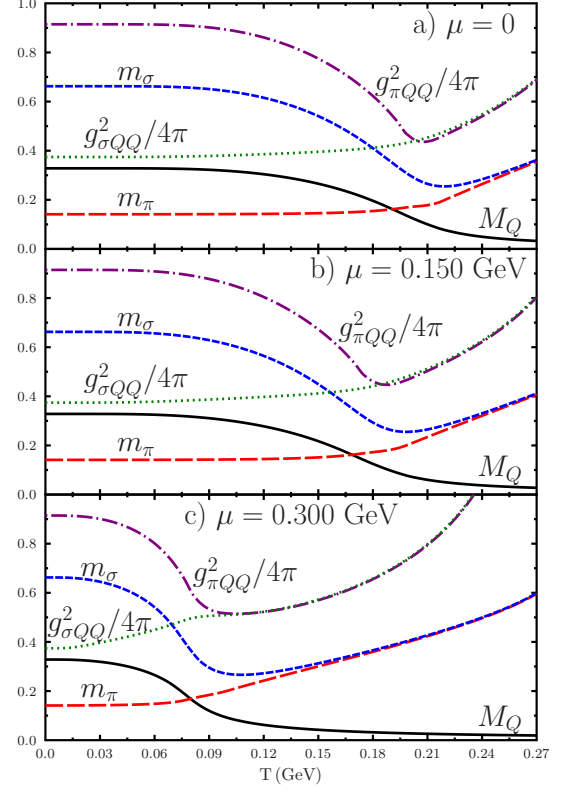


FIG. 1: The constituent quark mass M_Q (black solid line), pion mass m_π (red long dashed line), sigma mass m_σ (blue short dashed line) in GeV, and the quark-meson couplings $g_{\sigma QQ}^2/4\pi$ (green dotted line) and $g_{\pi QQ}^2/4\pi$ (purple dash-dotted line) as a function of T for three different values of chemical potential μ .

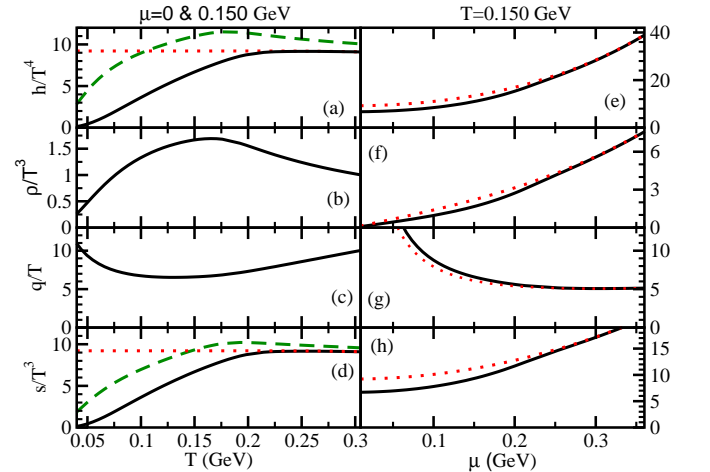


FIG. 2: Dimensionless ratios to the appropriate powers of T of the thermodynamical functions h , ρ , q , and s . Left panel: T dependence for $\mu = 0$ (dashed green) and $\mu = 0.15 \text{ GeV}$ (solid black). Right Panel: μ dependence for $T = 0.15 \text{ GeV}$. Dotted red curves are the ratios calculated with $M_Q = 0$ (on the left panel, $\mu = 0$).

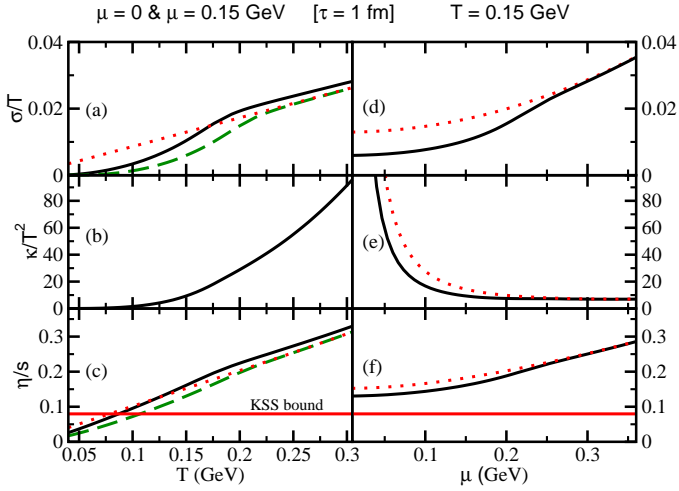


FIG. 3: T dependence of normalized electrical conductivity σ/T (a), thermal conductivity κ/T^2 (b) and shear viscosity η/s (c). Their μ dependence at $T = 0.150$ GeV are respectively in (d), (e) and (f). All results are obtained for $\tau = 1/\Gamma = 1$ fm. The (red) dotted lines are the results for massless quarks and the horizontal (red) solid line indicates the KSS holographic bound, $\eta/s = 1/4\pi$.

Next, we present our results for the transport coefficients. To get insight into the importance of using a thermal width $\Gamma_Q(\mathbf{k}, T, \mu)$ in which the $QQ \leftrightarrow QQ$ and $Q \leftrightarrow QM$ physical processes are treated consistently with the dynamics of chiral restoration, let us initially contrast results for the transport coefficients when one uses a (T, μ) -independent thermal width in Eqs. (16)-(18). We choose $\Gamma \equiv 1 \text{ fm}^{-1}$ —we often refer to the relaxation time, which is the inverse of the thermal width, $\tau = 1/\Gamma$. The results for a (T, μ) -independent $\Gamma(\mathbf{k}, T, \mu)$ are shown in Fig. 3, while those with the full (T, μ) dependence of $\Gamma(\mathbf{k}, T, \mu)$ are shown in Fig. 4. Clearly, they are markedly different. While the results in Fig. 3 are determined solely by phase space, those in Fig. 4 feature the interplay between smooth contributions from the $QQ \leftrightarrow QQ$ scattering processes (Sc, dotted lines) and Landau-cut cusp contribution from the $Q \leftrightarrow QM$ processes (LD, dashed lines). The results are easily understood examining in detail the Sc and LD contributions to the thermal widths, which we discuss next.

The temperature dependence of Γ and of its inverse τ is shown in Fig. 5 for two values of the chemical potential, $\mu = 0$ and $\mu = 0.15$ GeV. As can be seen in the figure, while the scattering (Sc) contribution is a smooth function of the temperature, the Landau-cut (LD) features a cusp at a critical temperature T_M , the Mott temperature. This is a threshold temperature beyond which $m_\pi(T \geq T_M) \geq 2M_Q(T \geq T_M)$, when the pionic bound state delocalizes into its constituents. The Mott temperature, although closely related to the chiral pseudocritical temperature discussed before, in the present model it is larger than the latter. In the chiral restored phase the system consists of a mixture of quarks and antiquarks

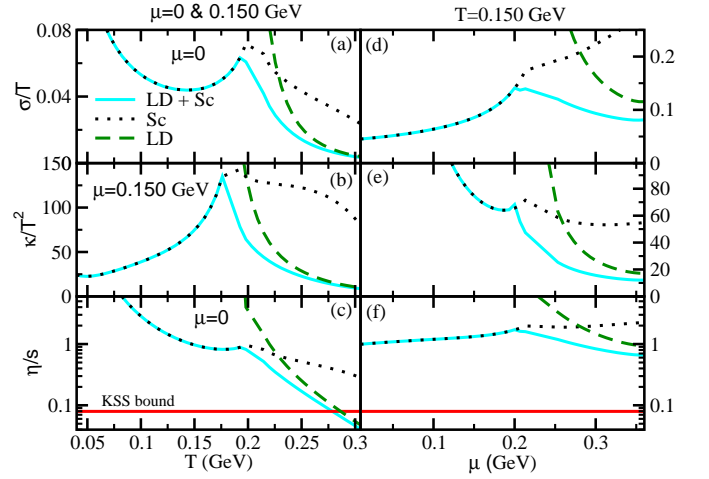


FIG. 4: (Color on-line) T dependence of σ/T (a), κ/T^2 (b) and η/s (c). Their μ dependence at $T = 0.150$ GeV are respectively in (d), (e) and (f). Contributions of LD (dashed line), Sc (dotted line) components and their total (solid line) in these transport coefficients are individually shown.

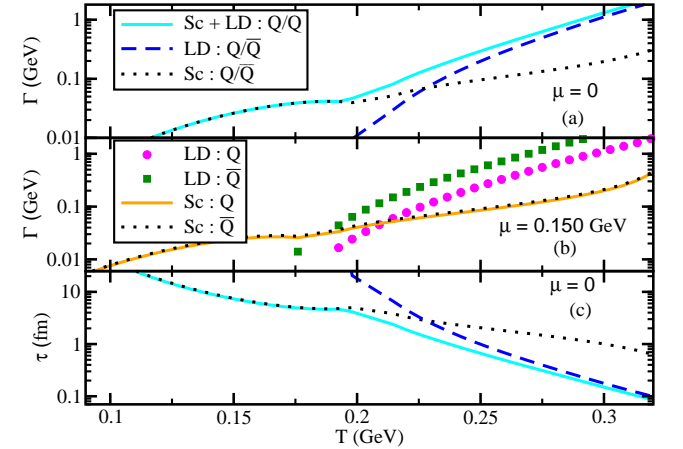


FIG. 5: (Color on-line) Contribution of Landau damping (LD) part (dashed line), $2 \leftrightarrow 2$ scattering part (solid line) and their total (dotted line) in the thermal widths (a) and relaxation times (c) of quark/anti-quark (Q/\bar{Q}) at $\mu = 0$. (b) at $\mu = 0.150$ GeV, circles and squares stand for LD part of thermal width for Q and \bar{Q} , while their scattering parts are plotted by solid and dotted lines.

and pions and for $T > T_M$ the pions as bound states disappear—for a thorough discussion on these temperatures, and their relation to the one of quark deconfinement, see e.g. Refs. [26, 54–56]. Therefore, below T_M , the LD contribution to the thermal width is zero. Beyond T_M , the thermal width gets strongly enhanced, meaning that quarks and antiquarks quickly thermalize in the medium. The figure also reveals that T_M decreases with μ . One can also identify a Mott chemical potential μ_M , as shown in Fig. 6. For $T = 0.150$ GeV, $\mu_M \sim 0.2$ GeV. Notice also that while the quark and anti-quark Sc and LD contributions are equal for $\mu = 0$, they are differ-

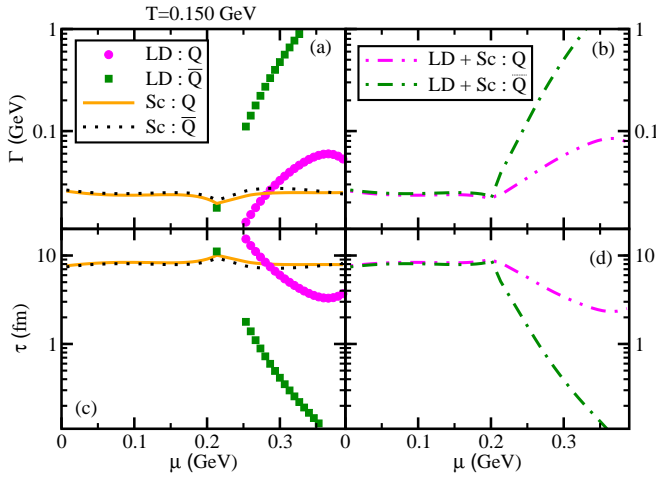


FIG. 6: (Color on-line) μ dependence of thermal widths (a) and relaxation times (c) for LD and scattering parts of quark and anti-quark. Their total thermal widths (b) and relaxation times (d) are plotted by dash-double dotted and dash-dotted lines.

ent at finite μ , a feature that is obviously due to the different dependence with μ of the quark and antiquark Fermi-Dirac distributions. We note that both quark and antiquark have the same T_M and μ_M , but they seem different in Figs. 5(b) and Fig. 6(a) because the quark contribution becomes too small close to threshold to become visible in those graphs. It is important to note that a cusp structure might not be present when using different set of model parameters which predict different values for the constituent-quark masses and quark-meson couplings. For example, Refs. [20, 25, 27] found a valley structure near the Mott transition temperature instead of a cusp structure.

Let us return to the transport coefficients. The η/s curve in Fig. 4 reveals interesting features. Below the chiral pseudocritical temperature, the magnitude of η/s is much larger than the KSS bound [51], $\eta/s = 1/4\pi$, shown by the horizontal red line in that figure, indicating that matter at those temperatures may not at all behave like a perfect fluid. However, beyond Mott temperature, η/s is abruptly reduced and approaches to KSS bound, crossing that bound at $T \sim 0.275$ GeV. The main cause for this behavior is the LD the contribution, which dominates the Sc contribution beyond the Mott temperature. We stress that at those high temperatures, there might exist additional contributions coming from gluonic degrees of freedom, which are not explicitly taken into account by the model and might raise the value of η/s . In the context of the present model, the message is that the LD contribution due to $Q \leftrightarrow QM$ inelastic scatterings in the medium is the origin of perfect fluid nature of quark matter near and above Mott temperature. The same is true for the electrical and thermal conductivities, they are also small for high values of T and μ due to a lower relaxation time of quarks due to inelastic scatterings.

V. SUMMARY AND CONCLUSIONS

In this work we have made a comparative study of the relative contributions of elastic $2 \leftrightarrow 2$ and inelastic $1 \leftrightarrow 2$ scatterings in electrical and thermal conductivities and shear viscosity of strongly interacting matter in the context of the NJL model. This is the first study taking into account both types of scatterings; previously, Refs. [17, 20–26, 29, 30] of effective QCD model calculations, Refs. [21–24, 29, 30] have estimated $1 \leftrightarrow 2$ type scattering like quark \leftrightarrow quark + meson by calculating quark self-energy for quark-meson loop at finite temperature. These $1 \leftrightarrow 2$ type scattering contribute within a very narrow temperature window, which is near but above Mott temperature. On the other hand, Refs. [17, 20, 25, 26] have investigated the contributions of $2 \leftrightarrow 2$ type scattering of quark in the transport coefficients, which contribute in entire temperature range. A simultaneous role of $2 \leftrightarrow 2$ and $1 \leftrightarrow 2$ type scatterings on transport coefficients has never been studied and the present work has provided such an investigation.

In the language of the Kubo formalism, the T and μ dependence of transport coefficients has two sources in this model. One is thermodynamical phase-space via the Fermi-Dirac distribution functions, which have explicit and implicit through the quark masses T and μ dependences. The other is via the thermal width, which is calculated here self-consistently with the dynamics of chiral restoration taking into account elastic and inelastic scatterings. The self-consistency has a dramatic effect on the transport coefficients, as we demonstrated by comparing the self-consistent results with those obtained with a constant thermal width. In this case, shear viscosity to entropy density ratio η/s and electrical conductivity to temperature ratio σ/T increase with both T and μ . Their rate of increments are changed when one approaches from hadron to quark phases in T - μ plane. Owing to the definition, thermal conductivity is generally diverged at $\mu = 0$ but its divergence is removed for finite μ . It rapidly decreases with μ because of thermodynamical quantity, enthalpy to net quark density ratio h/ρ , and then after $\mu = 0.150$ GeV, it remains more or less constant, whose strength is proportionally determined by relaxation time.

Next, an explicit T and μ dependence of thermal width of quark has been calculated from different quark-quark, quark-anti-quark elastic scatterings via meson exchanges and quark-meson in-elastic scatterings. All are in-medium scatterings and similarly, one can calculate anti-quark relaxation time by considering suitable diagrams. The in-elastic scatterings are estimated from imaginary part of quark self-energy due to quark-meson loops. Due to Mott effect, the quark meson in-elastic scattering has certain T - μ threshold, beyond which it becomes non-zero. However, elastic scatterings provide non-zero relaxation time in entire T - μ plane. Along the Mott curve or T_M - μ_M curve, it carries a mild cusp structure, which is also reflected in the (T, μ) profile of trans-

port coefficients. Adding elastic and in-elastic scatterings, we get total relaxation time of quark and anti-quark, for which we get very small η/s , close to its KSS bound. However, this possibility is expected near and above Mott curve in T - μ plane, where in-elastic scatterings suddenly blow up. Within this T - μ window, our outcome is supporting the picture of perfect fluid nature, observed in RHIC matter. Due to this lower relaxation time in this T - μ window, the other transport coefficients like electrical and thermal conductivities will also be small.

Acknowledgment: Work partially financed by by Conselho Nacional de Desenvolvimento Científico e Tecnológico - CNPq, 305894/2009-9 (G.K.), 464898/2014-5 (G.K) (INCT Física Nuclear e Aplicações), 168240/2017-3 (F.E.S), and Fundação de Amparo à Pesquisa do Estado de São Paulo - FAPESP, 2013/01907-0 (G.K). SG, AA, HM acknowledge Workshop in High Energy Physics Phenomenology (WHEPP), 2017 for getting some fruitful discussions on this work.

-
- [1] M. Buballa, V. Dexheimer, A. Drago, E. Fraga, P. Haensel, I. Mishustin, G. Pagliara, J. Schaffner-Bielich, S. Schramm, A. Sedrakian and F. Weber, J. Phys. G **41**, no. 12, 123001 (2014).
 - [2] G. Baym, T. Hatsuda, T. Kojo, P. D. Powell, Y. Song and T. Takatsuka, Rept. Prog. Phys. **81**, no. 5, 056902 (2018).
 - [3] E. L. Bratkovskaya, W. Cassing, P. Moreau and T. Song, KnE Energ. Phys. **3**, 234 (2018).
 - [4] E. Shuryak, Rev. Mod. Phys. **89**, 035001 (2017).
 - [5] R. Rapp Adv. High Energy Phys. 2013, 148253 (2013); R. Rapp, J. Wambach, Adv. Nucl. Phys. 25, 1 (2000).
 - [6] P. Mohanty, S. Ghosh, S. Mitra Adv. High Energy Phys. 2013, 176578 (2013).
 - [7] R. Arnaldi et al. Phys. Rev. Lett. **100**, 022302 (2008); R. Arnaldi et al., Eur. Phys. J. C **61**, 711 (2009); S. Damjanovic et al., J. Phys. G **35**, 104036 (2008).
 - [8] P. V. Buividovich, M. N. Chernodub, D. E. Kharzeev, T. Kalaydzhyan, E. V. Luschevskaya, and M. I. Polikarpov, Phys. Rev. Lett. **105**, 132001 (2010).
 - [9] A. Amato, G. Aarts, C. Allton, P. Giudice, S. Hands, J.I. Skullerud, Phys. Rev. Lett. **111**, 172001 (2013).
 - [10] Y. Burnier and M. Laine, Eur. Phys. J. C **72**, 1902 (2012).
 - [11] G. Aarts, C. Allton, J. Foley, S. Hands, and S. Kim, Phys. Rev. Lett. **99**, 022002 (2007).
 - [12] B. B. Brandt, A. Francis, H. B. Meyer, and H. Wittig, J. High Energy Phys. **03** (2013) 100.
 - [13] H.T. Ding, A. Francis, O. Kaczmarek, F. Karsch, E. Laermann, and W. Soeldner, Phys. Rev. D **83**, 034504 (2011).
 - [14] S. Gupta, Phys. Lett. B **597**, 57 (2004).
 - [15] C. Ratti, Rept. Prog. Phys. **81**, no. 8, 084301 (2018).
 - [16] D. Fernandez-Fraile and A. Gomez Nicola, Eur. Phys. J. C **62**, 37 (2009).
 - [17] R. Marty, E. Bratkovskaya, W. Cassing, J. Aichelin, and H. Berrehrah, Phys. Rev. C **88**, 045204 (2013).
 - [18] S. Gavin, Nucl. Phys. A **435**, 826 (1985).
 - [19] M. Prakash, M. Prakash, R. Venugopalan, and G. Welke, Phys. Rep. **227**, 321 (1993).
 - [20] P. Deb, G. P. Kadam, and H. Mishra, Phys. Rev. D **94**, 094002 (2016).
 - [21] S. Ghosh, T. C. Peixoto, V. Roy, F. E. Serna, and G. Krein, Phys. Rev. C **93**, 045205 (2016).
 - [22] S. Ghosh, A. Lahiri, S. Majumder, R. Ray, S. K. Ghosh, Phys. Rev. C **88**, 068201 (2013).
 - [23] R. Lang and W. Weise Eur. Phys. J. A **50**, 63 (2014).
 - [24] R. Lang, N. Kaiser, and W. Weise, Eur. Phys. J. A **51**, 127 (2015).
 - [25] P. Zhuang, J. Hufner, S.P. Klevansky, and L. Neise, Phys. Rev. D **51**, 3728 (1995).
 - [26] P. Rehberg, S.P. Klevansky, and J. Hufner, Nucl. Phys. A **608**, 356 (1996).
 - [27] C. Sasaki and K. Redlich, Nucl. Phys. A **832**, 62 (2010).
 - [28] A. Abhishek, H. Mishra, and S. Ghosh, Phys. Rev. D **97**, 014005 (2018).
 - [29] A. Harutyunyan, D. H. Rischke and A. Sedrakian, Phys. Rev. D **95**, no. 11, 114021 (2017).
 - [30] P. Singha, A. Abhishek, G. Kadam, S. Ghosh, and H. Mishra arXiv:1705.03084 [nucl-th].
 - [31] C. Lee and I. Zahed, Phys. Rev. C **90**, 025204 (2014).
 - [32] D. Fernandez-Fraile and A. Gomez Nicola, Phys. Rev. D **73**, 045025 (2006).
 - [33] S. Ghosh, Phys. Rev. D **95** (2017) 036018
 - [34] W. Cassing, O. Linnyk, T. Steinert, and V. Ozvenchuk, Phys. Rev. Lett. **110**, 182301 (2013).
 - [35] S. I. Finazzo and J. Noronha Phys. Rev. D **89**, 106008 (2014).
 - [36] A. Puglisi, S. Plumari, and V. Greco, Phys. Rev. D **90**, 114009 (2014); J. Phys. Conf. Ser. **612**, 012057 (2015); Phys. Lett. B **751**, 326 (2015).
 - [37] M. Greif, I. Bouras, Z. Xu, and C. Greiner, Phys. Rev. D **90**, 094014 (2014); J. Phys. Conf. Ser. **612**, 012056 (2015).
 - [38] D. Davesne, Phys. Rev. C **53**, 3069 (1996).
 - [39] S. Nam, Mod. Phys. Lett. A **30**, 1550054 (2015).
 - [40] M. Iwasaki and T. Fukutome, J. Phys. G **36**, 115012 (2009).
 - [41] S. Mitra and S. Sarkar, Phys. Rev. D **89** (2014) 054013; S. Mitra, U. Gangopadhyaya and S. Sarkar, Phys. Rev. D **91** (2015) 094012.
 - [42] I. A. Shovkovy and P. J. Ellis, Phys. Rev. C **66**, 015802 (2002).
 - [43] M. Braby, J. Chao, and T. Schäfer, Phys. Rev. C **81**, 045205 (2010).
 - [44] R. Kubo, J. Phys. Soc. Jap. **12**, 570 (1957).
 - [45] D. N. Zubarev *Non-equilibrium statistical thermodynamics* (New York, Consultants Bureau, 1974).
 - [46] P. Chakraborty and J. I. Kapusta, Phys. Rev. C **83**, 014906 (2011).
 - [47] M. Le Bellac, *Thermal Field Theory* (Cambridge University Press, Cambridge, England, 2000).
 - [48] S. Ghosh, Int. J. Mod. Phys. A **29**, 1450054 (2014).
 - [49] U. Vogl and W. Weise, Prog. Part. Nucl. Phys. **27**, 195 (1991); S. P. Klevansky, Rev. Mod. Phys. **64**, 649 (1992); T. Hatsuda and T. Kunihiro, Phys. Rep. **247**, 221 (1994); M. Buballa, Phys. Rep. **407**, 205 (2005).
 - [50] A. Hosoya, M.-A. Sakagami, and M. Takao, Ann. Phys. (N.Y.) **154**, 229 (1984).

- [51] P. Kovtun, D. T. Son and A. O. Starinets, Phys. Rev. Lett. **94**, 111601 (2005).
- [52] H.A. Weldon, Phys. Rev. D **D 28**, 2007 (1983).
- [53] E. Quack, S. P. Klevansky, Phys. Rev. **C 49**, 6 (1994).
- [54] H. Hansen, W. M. Alberico, A. Beraudo, A. Molinari, M. Nardi and C. Ratti, Phys. Rev. D **75**, 065004 (2007).
- [55] P. Costa, M. C. Ruivo, C. A. de Sousa, H. Hansen and W. M. Alberico, Phys. Rev. D **79**, 116003 (2009).
- [56] D. Blaschke, A. Dubinin and M. Buballa, Phys. Rev. D **91**, 125040 (2015).